Analysis of the Geodesic Interpolating Spline

A. M. Mills and T. Shardlow

School of Mathematics, The University of Manchester, Manchester M60 1QD, UK

May 2008

Image registration is the process of aligning desired features in two or more images, to which there are several approaches. We consider the approach of landmark-based pairwise registration considers registering two images, each with a set of landmarks marked, with a correspondence defined between the two sets of landmarks, where one of the images is to be registered to the other by a nonlinear warp so that the landmarks on the template image, T, are exactly aligned with with the corresponding landmarks on the reference image, R.

1 Introduction

Image registration is the process of aligning desired features in two or more images, to which there are several approaches, as described in [14]. We consider the approach of landmark-based pairwise registration which considers registering two images, each with a set of landmarks marked, with a correspondence defined between the two sets of landmarks, where one of the images is to be registered to the other by a nonlinear warp so that the landmarks on the template image, T, are exactly aligned with with the corresponding landmarks on the reference image, R.

We seek a warp, $\Phi : \Omega \to \Omega$, such that $\Phi(\mathbf{P}_i) = \mathbf{Q}_i, i = 1, \dots, n_c$, where $\mathbf{P}_i$ and $\mathbf{Q}_i$ for $i = 1, \dots, n_c$ are landmarks on, respectively the template image and the reference image, and where Ω is the domain of the images. To restrict the choice of Φ and make the problem well-defined, we choose Φ where the bending of the image is minimized, by using the Geodesic Interpolating Spline (GIS) [11].

We consider the Geodesic Interpolating Spline (GIS) for landmark registration. The clamped-plate spline [2] uses one large step, which can lead to folding or tearing in the image. To eliminate these problems, we introduce a time dependence to the registration. In this way, we will achieve a diffeomorphic mapping, by performing a concatenation of smaller warps rather than one large warp [3]. This is important as we do not wish to lose any information from the image, and for some implementations we require the mapping to be invertible. Problems involved in using non-invertible mappings are discussed in [7]. The necessity for mappings to be diffeomorphic is discussed in [8]. A similar method is defined for vector fields discretized on grids in [9].

We define a warp, Φ, in the following way. For a time dependent velocity field, $\mathbf{v}(\mathbf{x}, t) \in \mathbb{R}^d$ for $\mathbf{x} \in \Omega$ and $t \in [0, 1]$, let

$$\Phi(\mathbf{P}) = \mathbf{x}(1) \qquad \text{where } \frac{\mathrm{d}\mathbf{x}}{\mathrm{d}t} = \mathbf{v}(\mathbf{x}, t), \qquad \mathbf{x}(0) = \mathbf{P}, \tag{1.1}$$

where $\mathbf{P}$ is the set of initial knotpoints for the image.

Following [12], we develop a suitable method. The warp is defined by the deformation field, $\mathbf{v}$, found by solving the differential equation (1.3 *a*) in the minimization problem: minimize

$$l(\mathbf{x}_i(t), \mathbf{v}(t, \mathbf{x})) = \int_0^1 \int_\Omega \|L\mathbf{v}(t, \mathbf{x})\|^2 \mathrm{d}\mathbf{x}\, \mathrm{d}t, \tag{1.2}$$

over deformation fields, $\mathbf{v}(t, \mathbf{x}) \in \mathbb{R}^d$ and paths, $\mathbf{x}_i(t) \in \Omega$ for $i = 1, \dots, n_c$, where L is a constant-coefficient, differential operator, and such that

$$\frac{\mathrm{d}\mathbf{x}_i}{\mathrm{d}t} = \mathbf{v}(t, \mathbf{x}_i(t)), \qquad 0 \le t \le 1, \tag{1.3 a}$$

and

$$\mathbf{x}_i(0) = \mathbf{P}_i, \quad \text{and} \quad \mathbf{x}_i(1) = \mathbf{Q}_i, \qquad i = 1, \dots, n_c. \tag{1.3 b}$$

We have $\mathbf{P}_i$ and $\mathbf{Q}_i$ for $i = 1, \dots, n_c$ which are knotpoints on, respectively, the template image, T, and the reference image, R.

The differential operator, L in (1.2), is chosen to be ∇^2. This models the Willmore energy of the problem, known as the "bending energy". This operator comes from the modelling of the deformation of thin plates, as described in [5].

The Biharmonic Green's function is the natural choice of differential operator for the 2-dimensional case. A similar Green's function, the Triharmonic Green's function is available for the 3-dimensional case, but we restrict our consideration to the 2-dimensional case. We impose zero Dirichlet boundary conditions on the unit circle. These boundary conditions are satisfied by the Biharmonic Green's function derived by Boggio [1]:

$$G(\mathbf{x}, \mathbf{y}) = |\mathbf{x} - \mathbf{y}|^2 \left(\frac{1}{2}(A^2 - 1) - \ln A \right), \tag{1.4 a}$$

where

$$A(\mathbf{x}, \mathbf{y}) = \frac{\sqrt{|\mathbf{x}|^2 |\mathbf{y}|^2 - 2\mathbf{x}.\mathbf{y} + 1}}{|\mathbf{x} - \mathbf{y}|}, \tag{1.4 b}$$

where $\mathbf{x}$ and $\mathbf{y}$ are two-dimensional vectors.

This Green's function gives the required boundary conditions, as shown in [12]. The choice of operator and Green's function affects the success of the registration.

We show the existence of minimizing paths for the GIS and that the velocity field generated by a defined set of minimizing paths is unique. We show that this velocity field can be expanded as a finite linear combination of Green's functions without introducing any approximation. We describe the numerical solution methods used and investigate the homeomorphic and diffeomorphic properties of the mappings under numerical approximation. Finally, we consider conditions leading to non-unique minimizing paths.

2 Existence of minimizing paths and the uniqueness of corresponding velocity fields

We investigate the existence of minimizing paths and existence and uniqueness of the vector fields generated by such paths for the Geodesic Interpolating Spline problem. Based on the work of Dupuis, Grenander and Miller [6], we show the existence of minimizing paths and vector fields and uniqueness of the vector field generated by a given set of paths for the Geodesic Interpolating Spline. Dupuis, Grenander and Miller prove this result for inexact landmark registration, but we show that the analogous result holds in the case of exact landmark matching.

First we define the spaces that give the setting of the problem. We work in the space $V = L_2([0,1] : H \times \ldots \times H)$, where we have the d-times product, where d is typically 2 or 3, of the space

$$H = \{h \in H^2(\Omega) : h = 0 \text{ and } \frac{\partial h}{\partial \mathbf{n}} = 0 \text{ on } \partial\Omega\},$$

for the domain $\Omega \subset \mathbb{R}^d$, where Ω is smooth and bounded. The vector $\mathbf{n}$ is the unit normal on $\partial\Omega$ the boundary of the domain, Ω, and

$$H^2(\Omega) = \{\text{all distributions } h : \Omega \to \mathbb{R} \text{ such that } D^\alpha h \in L_2(\Omega), |\alpha| \leq 2\},$$

where $D^\alpha u$ represents all derivatives of total order $\leq \alpha$ and

$$L_2(\Omega) = \left\{ f : \Omega \to \mathbb{R} \text{ such that } \left(\int_\Omega |f(x)|^2 \mathrm{d}x \right)^{\frac{1}{2}} < \infty \right\}.$$

Define the norms

$$\|\mathbf{v}\|_V^2 = \sum_{k=1}^{d} \int_0^1 \|v_k(\cdot,t)\|_H^2 \mathrm{d}t, \qquad \text{for } \mathbf{v} = (v_1, \ldots, v_d) \in V, \qquad v_k(\cdot,t) \in H,$$

where

$$\|h\|_H^2 = \int_\Omega \|\triangle h\|_{\mathbb{R}^d}^2 \mathrm{d}\mathbf{x}, \qquad h \in H.$$

The space $C^1([s,t] : \Omega)$ is the set of continuous functions from $[s,t]$ to Ω with continuous first derivatives with norm defined by

$$\|f\|_{C^1([s,t]:\Omega)} = \sum_{j=0}^{1} \left\| \frac{\partial^j f}{\partial t^j} \right\|_{C([s,t]:\Omega)}$$

where

$$\|f\|_{C([s,t]:\Omega)} = \sup_{s \leq r \leq t} \|f(r)\|_{\mathbb{R}^d}.$$

The space $C^1(\Omega : \mathbb{R})$, abbreviated to $C^1(\Omega)$, is the space of continuous functions from Ω to $\mathbb{R}$ with continuous first derivatives. The corresponding norm is given by

$$\|f\|_{C^1(\Omega)} = \|f\|_{C(\Omega:\mathbb{R})} + \sum_{i=1}^{d} \left\| \frac{\partial f}{\partial x_i} \right\|_{C(\Omega:\mathbb{R})}$$

where

$$\|f\|_{C(\Omega:\mathbb{R})} = \sup_{\mathbf{x} \in \Omega} \|f(\mathbf{x})\|_{\mathbb{R}}.$$

Proposition 1 *Let $0 < \alpha < \frac{1}{2}$. Then there exists $C < \infty$ such that for all $\mathbf{f} \in H \times \ldots \times H$ and for all $\mathbf{x}, \mathbf{y} \in \Omega, d = 2, 3$*

$$\|\mathbf{f}(\mathbf{x}) - \mathbf{f}(\mathbf{y})\|_{\mathbb{R}^d} \leq C \|\mathbf{f}\|_{H \times \ldots \times H} |\mathbf{x} - \mathbf{y}|^\alpha. \tag{2.1}$$

Proof Working with the components, $f_k \in H, k = 1, \ldots, d$ of $\mathbf{f}$, the Compact Embedding Lemma states that there exists $C < \infty$ such that

$$|f_k(\mathbf{x}) - f_k(\mathbf{y})| \leq C\|f_k\|_H |\mathbf{x} - \mathbf{y}|^\alpha.$$

By definition of the $\mathbb{R}^d$ norm,

$$\begin{aligned}
\|\mathbf{f}(\mathbf{x}) - \mathbf{f}(\mathbf{y})\|_{\mathbb{R}^d} &= \left(\sum_{k=1}^{d} (f_k(\mathbf{x}) - f_k(\mathbf{y}))^2\right)^{\frac{1}{2}} \\
&\leq \left(\sum_{k=1}^{d} (C\|f_k\|_H |\mathbf{x} - \mathbf{y}|^\alpha)^2\right)^{\frac{1}{2}} \\
&\leq C|\mathbf{x} - \mathbf{y}|^\alpha \left(\sum_{k=1}^{d} \|f_k\|_H^2\right)^{\frac{1}{2}} \\
&\leq C\|\mathbf{f}\|_{H\times\ldots\times H} |\mathbf{x} - \mathbf{y}|^\alpha.
\end{aligned}$$

□

This gives us Hölder continuity for $\mathbf{f} \in H \times \ldots \times H$.

We show that minimizing paths and corresponding vector fields exist. We examine (control point) paths $\mathbf{x}_i \in C^1([0,1] : \Omega),\ i = 1, \ldots, n_c$ and deformation fields $\mathbf{v} \in V,\ \mathbf{v} = (v_1, \ldots, v_d),$ on $\mathbf{x} \in \Omega$, where n_c is the number of control points used.

Theorem 1 *We assume that there exists at least one deformation field,* $\mathbf{v} \in V$*, and control point paths,* $\mathbf{x}_i \in C^1([0,1] : \Omega)$*, such that*

$$\mathbf{x}_i(0) = \mathbf{P}_i, \qquad \mathbf{x}_i(1) = \mathbf{Q}_i, \qquad i = 1, \ldots, n_c, \tag{2.2}$$

where $\mathbf{P}_i$ *and* $\mathbf{Q}_i$ *give, respectively, the initial and final control point positions in* Ω*, and* $\mathbf{x}_i(t) \in \Omega$ *represents the control point path* $\mathbf{x}_i$ *at time* t*, conforming to the constraint*

$$\frac{\mathrm{d}\mathbf{x}_i(t)}{\mathrm{d}t} = \mathbf{v}(\mathbf{x}_i(t), t). \tag{2.3}$$

We describe such deformation fields and control paths as being in the feasible set

$$\mathcal{F} = \Big\{(\mathbf{v}, \{\mathbf{x}_i, i = 1, \ldots, n_c\}) \in V \times C^1([0,1] : \Omega)^{n_c} : (2.2) \textit{ and } (2.3) \textit{ hold}\Big\}.$$

Then there exist deformation fields and control point paths in the feasible set that minimize $\|\mathbf{v}\|_V^2$.

Proof By assumption, the feasible set is non-empty.

We begin by examining a sequence of deformation fields and paths, $(\mathbf{v}^n, \{\mathbf{x}_i^n, i = 1, \ldots, n_c\}) \in \mathcal{F}$ such that $\|\mathbf{v}^n\|_V \to \inf \|\mathbf{v}\|_V$ where the limit is over deformation fields and paths. Without loss of generality, in order to use the Banach-Alaoglu Theorem (see [17] for a statement of the theorem) to show convergence of a subsequence, we assume that the sequence is bounded above, so that we have

$$\|\mathbf{v}^n\|_V \leq M, \tag{2.4}$$

for some $M < \infty$.

By the Banach-Alaoglu Theorem we know that $\mathbf{v}^n$, a sequence of deformation fields in the feasible set, has a weakly convergent subsequence, $\mathbf{v}^{n_m} \in V$, so that we can write $\mathbf{v}^{n_m} \rightharpoonup \mathbf{v}^*$ for some weak limit $\mathbf{v}^* \in V$.

By weak lower semi-continuity of the norm, we have

$$\|\mathbf{v}^*\|_V^2 \le \liminf_{m\to\infty} \|\mathbf{v}^{n_m}\|_V^2. \tag{2.5}$$

We assume that there are paths $\mathbf{x}_i^*, i = 1, \ldots, n_c$ such that we have $(\mathbf{v}^*, \mathbf{x}_i^*, i = 1, \ldots, n_c) \in \mathcal{F}$ which will be shown later in the proof. With this assumption we see that

$$\|\mathbf{v}^*\|_V^2 \ge \liminf_{n\to\infty} \|\mathbf{v}^n\|_V^2, \tag{2.6}$$

since $\mathbf{v}^*$ with associated paths is always in the feasible set, so its norm must be greater than or equal to the infimum limit of the norm of the elements of the feasible set. Therefore, from (2.5) and (2.6), we have

$$\liminf_{n\to\infty} \|\mathbf{v}^n\|_V^2 = \liminf_{m\to\infty} \|\mathbf{v}^{n_m}\|_V^2 = \|\mathbf{v}^*\|_V^2, \tag{2.7}$$

so the sequence of deformation fields tends to the minimum.

We now examine the paths for the mappings. We want to show that we have a sequence of paths, $\mathbf{x}^n(s; t, \mathbf{x})$ such that

$$\begin{aligned} \dot{\mathbf{x}}^n(s; 1, \mathbf{x}) &= \mathbf{v}^n(\mathbf{x}^n(s; 1, \mathbf{x}), s) \\ \mathbf{x}^n(1; 1, \mathbf{x}) &= \mathbf{x}. \end{aligned} \tag{2.8}$$

We show that this sequence behaves such that $\mathbf{x}^n \to \mathbf{x}^*$ on $C^1([0,1] : \Omega)$, where $\mathbf{x}^*$ solves the ordinary differential equations

$$\begin{aligned} \dot{\mathbf{x}}^*(s; 1, \mathbf{x}) &= \mathbf{v}^*(\mathbf{x}^*(s; 1, \mathbf{x}), s) \\ \mathbf{x}^*(1; 1, \mathbf{x}) &= \mathbf{x}, \end{aligned} \tag{2.9}$$

the derivatives being taken with respect to s.

Before proceeding with the proof, we obtain an important result about the solution of (2.9).

Proposition 2 *Consider* $\mathbf{v} \in V$ *such that*

$$\|\mathbf{v}\|_V^2 < \infty.$$

Then for any $t \in [0,1]$ *and* $\mathbf{x} \in \bar{\Omega}$*, a solution to (2.9) exists.*

Proof The deformation field $\mathbf{v}$ is continuous, so standard theory of ordinary differential equations tells us that the solution exists. □

The system (2.9) gives us a flow across the whole domain. We only set constraints (2.2), (2.3) on the control point paths, but results that hold for the whole domain will apply to control point paths.

We take a control point, $\mathbf{x} \in \Omega$. In order to apply the Arzela-Ascoli theorem to our sequence of paths to show the existence of a convergent subsequence, we want to show $\{\mathbf{x}^n(\cdot;1,\mathbf{x})\}$ to be compact in $C([t-\delta,t+\delta]:\mathbb{R}^d)$ for small δ. We have

$$\|\mathbf{x}^n(t;1,\mathbf{x})-\mathbf{x}^n(s;1,\mathbf{x})\|_{\mathbb{R}^d} = \left\|\int_s^t \mathbf{v}^n(\mathbf{x}^n(r;t,\mathbf{x}),r)\mathrm{d}r\right\|_{\mathbb{R}^d} \tag{2.10}$$

$$\leq \int_s^t \|\mathbf{v}^n(\mathbf{x}^n(r;t,\mathbf{x}),r)\|_{\mathbb{R}^d}\mathrm{d}r \tag{2.11}$$

$$\leq \int_s^t \|\mathbf{v}^n(\cdot,r)\|_{C(\Omega:\mathbb{R}^d)}\mathrm{d}r. \tag{2.12}$$

Since H is continuously embedded in $C(\Omega:\mathbb{R})$ by the Sobolev Embedding Theorem we have, for some $A<\infty$,

$$\|\mathbf{v}^n(\cdot,r)\|_{C(\Omega:\mathbb{R}^d)} \leq A\|\mathbf{v}^n(\cdot,r)\|_{H\times\ldots\times H}. \tag{2.13}$$

Hence, we can write

$$\begin{aligned}\|\mathbf{x}^n(t;1,x)-\mathbf{x}^n(s;1,x)\|_{\mathbb{R}^d} &\leq A\int_s^t \|\mathbf{v}^n(\cdot,r)\|_{H\times\ldots\times H}\mathrm{d}r\\ &\leq A\int_0^1 1_{(s,t)}(r)\|\mathbf{v}^n(\cdot,r)\|_{H\times\ldots\times H}\mathrm{d}r,\end{aligned}$$

where

$$1_{(s,t)}(r) = \begin{cases} 1 & \text{if } r\in(\min(s,t),\max(s,t)) \\ 0 & \text{otherwise}\end{cases}.$$

Applying the Cauchy-Schwarz inequality and evaluating the first integral gives

$$\|\mathbf{x}^n(t;1,x)-\mathbf{x}^n(s;1,x)\|_{\mathbb{R}^d} \leq A(t-s)^{\frac{1}{2}}\left(\int_0^1 \|\mathbf{v}^n(\cdot,r)\|^2_{H\times\ldots\times H}\mathrm{d}r\right)^{\frac{1}{2}}. \tag{2.14}$$

Using (2.4), we conclude

$$\|\mathbf{x}^n(t;1,x)-\mathbf{x}^n(s;1,x)\|_{\mathbb{R}^d} \leq A(t-s)^{\frac{1}{2}}M.$$

This gives us Hölder continuity which gives us equicontinuity for the paths. In order to apply the Arzela-Ascoli Theorem, we also require our sequence to be bounded in the space $C([t-\delta,t+\delta]:\mathbb{R}^d)$. We now move to considering control point paths at time t, so we use the notation $\mathbf{x}_i^n(t), i=1,\ldots,n_c$ to denote the i-th control point path at time t. We have

$$\mathbf{x}_i^n(t) = \mathbf{P}_i + \int_0^t \mathbf{v}^n(\mathbf{x}_i^n(s),s)\mathrm{d}s.$$

So we can write

$$\|\mathbf{x}_i^n(t)\|_{\mathbb{R}^d} \leq \|\mathbf{P}_i\|_{\mathbb{R}^d} + \left\|\int_0^t \mathbf{v}^n(\mathbf{x}_i^n(s),s)\mathrm{d}s\right\|_{\mathbb{R}^d} \qquad \text{(by the triangle inequality).}$$

Examining the last term, we have

$$\begin{aligned}\left\|\int_0^t \mathbf{v}^n(\mathbf{x}_i^n(s),s)\mathrm{d}s\right\|_{\mathbb{R}^d} &\le \int_0^t \|\mathbf{v}^n(\cdot,s)\|_{C(\Omega:\mathbb{R})}\mathrm{d}s\\ &\le A\int_0^t \|\mathbf{v}^n(\cdot,s)\|_{H\times\ldots\times H}\mathrm{d}s\\ &\le A\|\mathbf{v}^n\|_V.\end{aligned}$$

Since we assume that the sequence $\mathbf{v}^n$ is bounded above (2.4) in the norm $\|\cdot\|_V$, we see that the sequence $\mathbf{x}^n$ is bounded above in the norm $\|\cdot\|_{\mathbb{R}^d}$. Recalling that our domain is compact, we are able to apply the Arzela-Ascoli theorem, so that we can write a convergent subsequence of $\mathbf{x}^n$ as ϕ^n with limit ϕ^*.

Adding and subtracting terms, we can write

$$\begin{aligned}\int_t^1(\mathbf{v}^n(\phi^n(s),s)-\mathbf{v}^*(\phi^*(s),s))\mathrm{d}s &= \int_t^1(\mathbf{v}^n(\phi^n(s),s)-\mathbf{v}^n(\phi^*(s),s))\mathrm{d}s\\ &\quad+\int_t^1(\mathbf{v}^n(\phi^*(s),s)-\mathbf{v}^*(\phi^*(s),s))\mathrm{d}s. \qquad (2.15)\end{aligned}$$

By Proposition 1, we can estimate the first term of (2.15) as follows, applying the Cauchy-Schwarz inequality as in (2.14)

$$\int_t^1(\mathbf{v}^n(\phi^n(s),s)\;-\;\mathbf{v}^n(\phi^*(s),s))\mathrm{d}s \qquad (2.16)$$

$$\begin{aligned}&\le (1-t)^{\frac{1}{2}}\left(\int_0^1 C\|\mathbf{f}\|_{H\times\ldots\times H}\|\phi^n(s)-\phi^*(s)\|^2_{\mathbb{R}^d}\alpha\mathrm{d}s\right)^{\frac{1}{2}}\\ &\le C\|\phi^n(s)-\phi^*(s)\|^\alpha_{C([0,1]:\mathbb{R}^d)}\\ &\to 0 \text{ since } \phi^n \text{ is a convergent subsequence with limit } \phi^*.\end{aligned}$$

To examine the second term, we use the weak convergence of $\mathbf{v}^n$ to $\mathbf{v}^*$ in $C([0,1]:\Omega)$. We can write $\mathbf{w}^n=\mathbf{v}^n-\mathbf{v}^*\rightharpoonup 0$ and define the function $\mathbf{z}^n\in C(\Omega\times[0,1]:\mathbb{R}^d)$ as

$$\mathbf{z}^n(\cdot,t)=\int_t^1\mathbf{w}^n(\cdot,s)\mathrm{d}s. \qquad (2.17)$$

In order to apply the Arzela-Ascoli theorem, we show $\mathbf{z}^n$ to be bounded and equicontinuous on $C(\Omega\times[0,1]:\mathbb{R}^d)$. With $0\le s\le t\le 1$ and $\mathbf{x},\mathbf{y}\in\Omega$, we have

$$\begin{aligned}\|\mathbf{z}^n(\mathbf{x},t)-\mathbf{z}^n(\mathbf{y},s)\|_{\mathbb{R}^d} &\le \left\|\int_t^1(\mathbf{w}^n(\mathbf{x},r)-\mathbf{w}^n(\mathbf{y},r)\mathrm{d}r\right\|_{\mathbb{R}^d}\\ &\quad+\left\|\int_s^t\mathbf{w}^n(\mathbf{y},r)\mathrm{d}r\right\|_{\mathbb{R}^d} \qquad (2.18)\\ &\le C\|\mathbf{x}-\mathbf{y}\|^\alpha_{\mathbb{R}^d}+(t-s)^{\frac{1}{2}}\|\mathbf{w}^n\|_V, \qquad (2.19)\end{aligned}$$

using Proposition 1. By the construction of $\mathbf{v}^n$, $\|\mathbf{w}^n\|_V$ is bounded, and the sequence $\mathbf{z}^n$ is equicontinuous.

We have

$$\begin{aligned}\|\mathbf{z}^n(\mathbf{x},t)\|_{\mathbb{R}^d} &\leq \|\mathbf{z}^n(\mathbf{x},1)\|_{\mathbb{R}^d} + \|\mathbf{z}^n(\mathbf{x},1)-\mathbf{z}^n(\mathbf{x},t)\|_{\mathbb{R}^d}\\ &\leq A(1-t)^{\frac{1}{2}}\|\mathbf{w}^n\|_V\end{aligned}$$

as $\mathbf{z}^n(\mathbf{x},1)=0$. So the sequence is bounded.

Hence, by the Arzela-Ascoli theorem, we have $\mathbf{z}^n \to \mathbf{z}^*$ for some limit point $\mathbf{z}^* \in C(\Omega\times[0,1]:\mathbb{R}^d)$. Since $\mathbf{w}^n \to 0$ in V, we have

$$\int_\Omega\int_0^1 \Big\langle \boldsymbol{\gamma}(\mathbf{x},s), \mathbf{w}^n(\mathbf{x},s)\Big\rangle_{\mathbb{R}^d} \mathrm{d}s\,\mathrm{d}\mathbf{x} \to 0 \qquad \forall \boldsymbol{\gamma}\in V.$$

In particular, if $\boldsymbol{\gamma}(\mathbf{x},s)=\boldsymbol{\gamma}(\mathbf{x})1_{\{s\geq t\}}$, where

$$1_{\{s\geq t\}} = \begin{cases} 1 & \text{if } s\geq t\\ 0 & \text{otherwise}\end{cases},$$

then we have

$$\int_\Omega \Big\langle \boldsymbol{\gamma}(\mathbf{x}), \int_t^1 \mathbf{w}^n(\mathbf{x},s)\mathrm{d}s\Big\rangle_{\mathbb{R}^d}\mathrm{d}\mathbf{x}\to 0.$$

Using

$$\mathbf{z}^n(\mathbf{x},t) = \int_t^1 \mathbf{w}^n(\mathbf{x},s)\mathrm{d}s,$$

we obtain

$$\int_\Omega \Big\langle \boldsymbol{\gamma}(\mathbf{x}), \mathbf{z}^n(\mathbf{x},t)\Big\rangle_{\mathbb{R}^d}\mathrm{d}\mathbf{x}\to 0.$$

Since this holds for all $\boldsymbol{\gamma}\in C(\Omega:\mathbb{R}^d)$, we know $\mathbf{z}^*=0$. So we have shown

$$\int_t^1 (\mathbf{v}^n(\mathbf{x},s)-\mathbf{v}^*(\mathbf{x},s))\mathrm{d}s \to 0 \qquad \text{as } n\to\infty,\ \forall \mathbf{x}\in\Omega. \tag{2.20}$$

To show that the second term of (2.15) tends to zero, we deal with two cases. In the particular case that we have $\phi^*(s)=\mathbf{x}$ and fixed $\mathbf{x}\in\Omega$, clearly the second term tends to zero. In the general case we can write, adding and subtracting terms appropriately,

$$\begin{aligned}\int_t^1 \mathbf{v}^n(\phi^*(s),s)-\mathbf{v}^*(\phi^*(s),s)\mathrm{d}s &= \int_t^1 \mathbf{v}^n(\phi^*(s),s)-\mathbf{v}^n(\phi^m(s),s)\mathrm{d}s\\ &+\int_t^1 \mathbf{v}^n(\phi^m(s),s)-\mathbf{v}^*(\phi^m(s),s)\mathrm{d}s + \int_t^1 \mathbf{v}^*(\phi^m(s),s)-\mathbf{v}(\phi^*(s),s)\mathrm{d}s.\end{aligned} \tag{2.21}$$

We can use similar arguments to those used in (2.16), to write

$$\begin{aligned}\left\|\int_t^1 \mathbf{v}^n(\phi^*(s),s)-\mathbf{v}^n(\phi^m(s),s)\mathrm{d}s\right\|_{\mathbb{R}^d} &\leq \int_t^1 \|\mathbf{v}^n(\phi^*(s),s)-\mathbf{v}^n(\phi^m(s),s)\|_{\mathbb{R}^d}\mathrm{d}s\\ &\leq C\int_t^1 \|\phi^*(s)-\phi^m(s)\|^\alpha_{\mathbb{R}^d}\mathrm{d}s,\end{aligned} \tag{2.22}$$

where α and C are the constants from Hölder continuity. Hence the first term of (2.21) tends to zero as $n\to\infty$. Similarly the third term of (2.21) tends to zero as $n\to\infty$.

Examining the second term of (2.21), we introduce a sequence of piecewise constant approximations ϕ^m to ϕ^* such that

$$\phi^*(s) = \lim_{m\to\infty} \phi^m(s), \qquad \forall s \in [t,1].$$

Let the elements of the sequence be constructed in the following way,

$$\phi^m(s) = \begin{cases} a_1, & s \in (t, t+\epsilon_1) \\ a_2, & s \in (t+\epsilon_1, t+\epsilon_1+\epsilon_2) \\ \vdots & \vdots \\ a_q, & s \in (t+\sum_{i=1}^{q-1}\epsilon_i, 1), \end{cases}$$

where the function takes q constant, not necessarily distinct, values $a_1, \ldots, a_q \in \Omega$ over intervals of length $\epsilon_1, \ldots, \epsilon_q$. So we have for the second term of (2.21)

$$\int_t^1 (\mathbf{v}^n(\phi^m(s), s) - \mathbf{v}^*(\phi^m(s), s))\mathrm{d}s = \int_t^{t+\epsilon_1} (\mathbf{v}^n(a_1, s) - \mathbf{v}^*(a_1, s))\mathrm{d}s + \ldots + \int_{t+\sum_{i=1}^{q-1}\epsilon_i}^1 (\mathbf{v}^n(a_q, s) - \mathbf{v}^*(a_q, s))\mathrm{d}s.$$

So by (2.20), we see that the second term of (2.21) tends to zero as $n \to \infty$, since all arguments to $\mathbf{v}^*$ and $\mathbf{v}^n$ are constant. Hence we conclude for all $t \in [0,1]$,

$$\int_t^1 (\mathbf{v}^n(\phi^n(s), s) - \mathbf{v}^*(\phi^*(s), s))\mathrm{d}s \to 0 \qquad \text{as } n \to \infty$$

and therefore we have

$$\begin{aligned} \phi^*(t) = \lim_{n\to\infty} \phi^n(t) &= \lim_{n\to\infty} \int_t^1 \mathbf{v}^n(\phi^n(s), s)\mathrm{d}s + \mathbf{x} \\ &= \int_t^1 \mathbf{v}^*(\phi^*(s), s)\mathrm{d}s + \mathbf{x}. \end{aligned}$$

Differentiating with respect to t,

$$\mathbf{v}^*(\phi^*(t), t) = \frac{\mathrm{d}\phi^*(t)}{\mathrm{d}t},$$

which shows that $\phi^*(t)$ conforms to the required constraint, since letting $\phi^*(t) = \mathbf{x}_i^*(t)$ gives

$$\frac{\mathrm{d}\mathbf{x}_i^*(t)}{\mathrm{d}t} = \mathbf{v}^*(\mathbf{x}_i^*(t), t).$$

Since ϕ^n is a convergent subsequence of $\mathbf{x}^n$, and $\sup_{0\le t\le 1} |\phi^n(t) - \phi^*(t)| \to 0$ as $n \to \infty$, we have $\phi^n(0) = \mathbf{P}_i$, $\phi^n(1) = \mathbf{Q}_i$.

Hence we see that there exist deformation fields and control point paths in the feasible set that minimize $\|\mathbf{v}\|_V^2$. □

3 Representation as a finite linear combination of Green's functions

We define the representative of a functional and show that the velocity field can be expanded as a finite linear combination of Green's functions with zero Dirichlet boundary conditions without introducing any approximation.

Theorem 2 *Riesz Representation Theorem - To each bounded linear functional, Φ on a Hilbert space $\mathcal{H}$, there corresponds an element $u \in \mathcal{H}$ such that*

$$\Phi(f) = \langle f, u \rangle_{\mathcal{H}} \qquad \forall f \in \mathcal{H}.$$

The element u is called the representative of Φ in $\mathcal{H}$.

Theorem 3 *Cheney and Light (see [4] for proof) - Let $\Phi_1, \dots, \Phi_{n_c}$ be continuous linear functionals on a Hilbert space, $\mathcal{H}$. Suppose we have, for some unknown element, $\mathbf{f}$, a set of numerical values $\Phi_1(\mathbf{f}), \dots, \Phi_{n_c}(\mathbf{f})$. Then $\mathbf{f}$ can be any element in the manifold $M = \{\mathbf{m} \in \mathcal{H} : \Phi_i(\mathbf{m}) = \Phi_i(\mathbf{f}), 1 \le i \le n_c\}$.*

Suppose $\mathbf{v}_{min}$ is the element of M with minimal norm, known as the minimal norm interpolant*. Then for $Y = \{\mathbf{y} \in \mathcal{H} : \Phi_i(\mathbf{y}) = 0, 1 \le i \le n_c\}$, we have $\mathbf{v}_{min} \perp Y$.*

We adapt a theorem taken from Cheney and Light [4] to show that the velocity fields can be expanded in terms of their representatives.

Theorem 4 *Let $\Phi_1, \dots, \Phi_{n_c}$ be continuous linear functionals on a Hilbert space, $\mathcal{H}$, with representatives $u_1, \dots, u_{n_c} \in \mathcal{H}$ respectively. Suppose for some unknown element $h \in \mathcal{H}$, we have values $\Phi_1(h), \dots, \Phi_{n_c}(h)$. Then h is some element of the manifold $M = \{m \in \mathcal{H} : \Phi_i(m) = \Phi_i(h), 1 \le i \le n_c\}$. Suppose h_{min} is the element with minimal norm, the minimal norm interpolant. Then $h_{min} = \sum_{j=1}^{n_c} \alpha_j u_j$, where the coefficients α_j solve the system of linear equations*

$$\sum_{j=1}^{n_c} \alpha_j \langle u_i, u_j \rangle = \langle h, u_i \rangle. \tag{3.1}$$

Proof Let

$$\begin{aligned} Y &= \{\mathbf{y} \in \mathcal{H} : \Phi_i(\mathbf{y}) = 0, 1 \le i \le n_c\} \\ &= \{\mathbf{y} \in \mathcal{H} : \langle \mathbf{y}, u_i \rangle = 0, 1 \le i \le n_c\} \\ &= \bigcap_{i=1}^{n_c} u_i^{\perp}. \end{aligned}$$

Now, $h_{\min}$ is characterized by the properties $h_{\min} \perp Y$ (from Theorem 3) and $\Phi_i(h_{\min}) = \Phi_i(h)$ for $1 \le i \le n_c$. Since $h_{\min} \in (\bigcap_{i=1}^{n_c} u_i^{\perp})^{\perp}$, we can infer that $h_{\min} \in \operatorname{span}\{u_1, \dots, u_{n_c}\}$. Writing $h_{\min} = \sum_{j=1}^{n_c} \alpha_j u_j$, we have

$$\Phi_i(h) = \Phi_i(h_{\min}) = \sum_{j=1}^{n_c} \alpha_j \Phi_i(u_j) \qquad (1 \le i \le n_c).$$

Thus the coefficients α_j solve the system of linear equations (3.1) described. $\square$

In Theorem 1, we have shown that a solution to the minimization problem $\min_{\mathbf{x}_i, \mathbf{v}} \|\mathbf{v}\|_V^2$ exists. Now we show that the velocity field in the solution can be represented as a finite linear combination of Green's functions.

Theorem 5 *The solution* $\mathbf{v}$ *to the problem of Theorem 1 can be written in the form*

$$\mathbf{v}(\mathbf{x}, t) = \sum_{i=1}^{n_c} \boldsymbol{\alpha}_i(t) G(\mathbf{x}_i(t), \mathbf{x}),$$

where $G(\cdot, \cdot)$ *is a Green's function with zero Dirichlet boundary conditions with coefficients* $\boldsymbol{\alpha}_i(t) \in \mathbb{R}^d$.

Proof We apply Theorem 4 in our case. We define a set of continuous linear functionals on H for fixed $k \in 1, \ldots, d$ so that we examine one row of the representation, for fixed time, t as

$$\Phi_i(h) = h(\mathbf{P}_i) \qquad i = 1, \ldots, n_c,\ \Phi_i \in H,\ h \in H, \tag{3.2}$$

where $(\mathbf{P}_1, \ldots, \mathbf{P}_{n_c})$ is the set of initial control point positions. We know Φ_i to be linear and continuous and hence bounded. Therefore we know by the Riesz Representation Theorem (Theorem 2) that there exists some representative u_i of Φ_i in H so that

$$\Phi_i(h) = \langle u_i, h \rangle_H \qquad \forall h \in H, \tag{3.3}$$

where $\langle \cdot, \cdot \rangle_H$ denotes the inner product on H.

We introduce a Green's function, $G(\mathbf{x}, \mathbf{y})$ which behaves so that

$$\triangle^2 G(\mathbf{x}, \mathbf{y}) = \delta(\mathbf{x} - \mathbf{y}).$$

We use the biharmonic Green's function, as described in the introduction. We know this Green's function to be in $L_2(\Omega)$ with first and second order derivatives in $L_2(\Omega)$. This Green's function also has zero Dirichlet boundary conditions. Hence we see that the Green's function is in H, as described in Section 2. Let $u_i(\mathbf{x}) = G(\mathbf{x}, \mathbf{P}_i)$. Then

$$\triangle^2 u_i(\mathbf{x}) = \delta(\mathbf{x} - \mathbf{P}_i).$$

We have

$$\begin{aligned}
\langle G(\cdot, \mathbf{P}_i), h \rangle_H &= \langle \delta(\cdot - \mathbf{P}_i), h \rangle_{L_2}, \qquad h \in H \\
&= \int_\Omega \delta(\cdot - \mathbf{P}_i) h(\cdot) \mathrm{d}\mathbf{x} \\
&= h(\mathbf{P}_i) \qquad \text{(by the sifting property of the } \delta\text{−function).}
\end{aligned}$$

We have shown $G(\cdot, \mathbf{P}_i)$ to be a representative for Φ_i in H. Hence we see that $G(\cdot, \mathbf{P}_1)$, …, $G(\cdot, \mathbf{P}_{n_c}) \in H$ are representatives for $\Phi_1, \ldots, \Phi_{n_c}$ in H. We now apply this result for the space, H, to the space, V.

We have the minimum norm interpolant $\mathbf{v}_{min} = (v_1(\cdot, t), \ldots, v_d(\cdot, t)) \in V$. So $\mathbf{v}_{min}$ minimizes $\|\mathbf{v}\|_V^2$, such that the interpolation conditions (3.4) hold. From the velocity constraint (2.3), we have interpolation conditions given by

$$\mathbf{v}(\mathbf{x}_i(t), t) = \frac{\mathrm{d}\mathbf{x}_i(t)}{\mathrm{d}t}, \tag{3.4}$$

when we know the paths $\mathbf{x}_i(t)$.

By definition of the norm on V, we have

$$\begin{aligned}\|\mathbf{v}\|_V^2 &= \int_0^1 \|\mathbf{v}(\cdot,t)\|^2_{H\times\ldots\times H}\mathrm{d}t\\ &= \sum_{k=1}^d \int_0^1 \|v_k(\cdot,t)\|_H^2\mathrm{d}t.\end{aligned}$$

Examining the elements of $\mathbf{v}$ we observe that we can separate component-wise, both in terms of time and knotpoints. Hence we see that if $\mathbf{v}_{min}$ is a minimum on V, the element $v_k(\cdot,t),\ k=1,\ldots,d$ minimizes

$$\|v_k(\cdot,t)\|_H^2$$

such that

$$\frac{\mathrm{d}x_{i,k}(t)}{\mathrm{d}t} = v_k(\mathbf{x}_i(t),t),$$

where the paths $\mathbf{x}_i(t) = (x_{i,1}(t),\ldots,x_{i,d}(t))$ are known so that the left hand side of the above represents the known values as in Theorem 4.

Hence we see that $v_k(\cdot,t)$ is in the appropriate manifold, M, for the problem, given by $M = \{v_k(\cdot,t)\in\mathcal{H} : \frac{\mathrm{d}x_{i,k}(t)}{\mathrm{d}t} = v_k(\mathbf{x}_i(t),t), 1\le i\le n_c\}$ and we have shown $v_k(\cdot,t)$ to be the element of the manifold with minimal norm.

Hence, by Theorem 4, we see that we can represent the elements $v_k,\ k=1,\ldots,d$ of $\mathbf{v}_{min}$ as

$$v_k(\cdot,t) = \sum_{i=1}^{n_c}\alpha_{i,k}(t)G(\cdot,\mathbf{x}_i),$$

where we have $\boldsymbol{\alpha}_i(t) = (\alpha_{i,1}(t),\ldots,\alpha_{i,d}(t))$.

Therefore we can represent the minimum norm interpolant of $\mathbf{v}$ as

$$\mathbf{v}_{\min}(\mathbf{x},t) = \sum_{i=1}^{n_c}\boldsymbol{\alpha}_i(t)G(\mathbf{x}_i(t),\mathbf{x}). \tag{3.5}$$

□

This expansion gives us the velocity field in a form convenient for implementation without introducing any approximation.

4 Numerical Methods

We restate the Geodesic Interpolating Spline problem in a Hamiltonian dynamics framework, and solve numerically. Methods for computation of the solution to the problem are discussed further in [13].

Using the representation for the velocity field from (3.5), the Geodesic Interpolating Spline problem can be written as

$$\min\int_0^1 \frac{1}{2}\sum_{i,j=1}^{n_c}\boldsymbol{\alpha}_i^\top\boldsymbol{\alpha}_j G(\mathbf{q}_i,\mathbf{q}_j)\mathrm{d}t \tag{4.1 a}$$

such that

$$\frac{\mathrm{d}\mathbf{q}_i}{\mathrm{d}t} = \sum_{j=1}^{n_c} \boldsymbol{\alpha}_j G(\mathbf{q}_i, \mathbf{q}_j), \qquad \mathbf{q}_i(0) = \mathbf{P}_i \qquad i = 1, \ldots, n_c, \tag{4.1 b}$$

where (4.1 b) gives the velocity constraint and $\mathbf{P}_i$ is a set of knotpoints on the image to which the warp is to be applied.

We can treat this as a Lagrangian by setting

$$L(\mathbf{q}, \dot{\mathbf{q}}) = \frac{1}{2} \sum_{i,j=1}^{n_c} \boldsymbol{\alpha}_i^\top \boldsymbol{\alpha}_j G(\mathbf{q}_i, \mathbf{q}_j), \tag{4.2}$$

where $\mathbf{q} = (\mathbf{q}_1, \ldots, \mathbf{q}_{n_c})$ and $\dot{\mathbf{q}} = (\dot{\mathbf{q}}_1, \ldots, \dot{\mathbf{q}}_{n_c}) = (\frac{\mathrm{d}\mathbf{q}_1}{\mathrm{d}t}, \ldots, \frac{\mathrm{d}\mathbf{q}_{n_c}}{\mathrm{d}t})$ represent position and velocity respectively. We see that the Hamiltonian of the system is the Legendre transform of the Lagrangian function as a function of the velocity $\dot{\mathbf{q}}$. The generalized momentum is given by

$$\frac{\partial L}{\partial \dot{\mathbf{q}}} = \mathcal{G}^{-1}\mathcal{G}\boldsymbol{\alpha} = \boldsymbol{\alpha}. \tag{4.3}$$

Hence, we have the coupled system of Hamiltonian equations

$$\dot{\mathbf{q}} = \frac{\partial H}{\partial \boldsymbol{\alpha}}, \tag{4.4 a}$$

$$\dot{\boldsymbol{\alpha}} = -\frac{\partial H}{\partial \mathbf{q}}. \tag{4.4 b}$$

with initial conditions

$$\begin{bmatrix} \mathbf{q}(0) \\ \boldsymbol{\alpha}(0) \end{bmatrix} = \begin{bmatrix} \mathbf{P} \\ \mathbf{A} \end{bmatrix} = \mathbf{Y}, \tag{4.5}$$

where $\mathbf{P}$ is the vector of initial knotpoint positions in (4.1 b) and $\mathbf{A}$ is the initial vector of generalized momentum.

The system (4.1 a),(4.1 b) is equivalent to the nonlinear system of equations $\Phi(\mathbf{A};\mathbf{P}) = \mathbf{Q}$ which we solve for $\mathbf{A}$ as a shooting problem, where $\Phi(\mathbf{A};\mathbf{P}) := \mathbf{q}(1)$, the position component of the solution of the Hamiltonian system

$$\frac{\mathrm{d}}{\mathrm{d}t}\mathbf{q}_i = \sum_{j=1}^{n_c} \boldsymbol{\alpha}_j G(\mathbf{q}_i, \mathbf{q}_j), \tag{4.6}$$

$$\frac{\mathrm{d}}{\mathrm{d}t}\boldsymbol{\alpha}_i = -\sum_{j=1}^{n_c} \boldsymbol{\alpha}_i^\top \boldsymbol{\alpha}_j \frac{\partial}{\partial \mathbf{q}_j} G(\mathbf{q}_i, \mathbf{q}_j),\ i = 1, \ldots, n_c, \tag{4.7}$$

with initial conditions given in (4.5).

To solve (4.6) and (4.7), we discretize in time. We choose to discretize using the Forward Euler method. Experiments with symplectic methods have shown no advantage for this problem, principally because it is a boundary value problem where long time simulations are not of interest, and no suitable explicit symplectic integrators are available [10]. Using the notation $\mathbf{q}_i^n \approx \mathbf{q}_i(n\Delta t)$, $\boldsymbol{\alpha}_i^n \approx \boldsymbol{\alpha}_i(n\Delta t)$, $n = 0, \ldots, N$, $\Delta t = 1/N$, we have

$$\begin{bmatrix} \mathbf{q}^{n+1} \\ \boldsymbol{\alpha}^{n+1} \end{bmatrix} = \begin{bmatrix} \mathbf{q}^n \\ \boldsymbol{\alpha}^n \end{bmatrix} + \Delta t \begin{bmatrix} \frac{H(\mathbf{q}^n, \boldsymbol{\alpha}^n)}{\partial \boldsymbol{\alpha}} \\ -\frac{H(\mathbf{q}^n, \boldsymbol{\alpha}^n)}{\partial \mathbf{q}} \end{bmatrix}, \qquad \begin{bmatrix} \mathbf{P} \\ \mathbf{A} \end{bmatrix} = \begin{bmatrix} \mathbf{q}^0 \\ \boldsymbol{\alpha}^0 \end{bmatrix} = \mathbf{Y}\ . \tag{4.8}$$

We wish to examine the variation with respect to the initial momentum, $\mathbf{A}$ in order to provide Jacobians for the nonlinear solver. The initial positions, $\mathbf{P}$ remain fixed. Using the Forward Euler scheme for some function $\mathbf{f}$, we have $\mathbf{X}^{n+1} = \mathbf{X}^n + \Delta t \mathbf{f}(\mathbf{X}^n)$ with initial condition $\mathbf{X}^0 = \mathbf{Y}$. Differentiating with respect to $\mathbf{A}$ gives

$$\frac{\mathrm{d}\mathbf{X}^{n+1}}{\mathrm{d}\mathbf{A}} = \frac{\mathrm{d}\mathbf{X}^n}{\mathrm{d}\mathbf{A}} + \Delta t \frac{\mathrm{d}\mathbf{f}(\mathbf{X}^n)}{\mathrm{d}\mathbf{X}^n}\frac{\mathrm{d}\mathbf{X}^n}{\mathrm{d}\mathbf{A}}, \qquad \frac{\mathrm{d}\mathbf{X}^0}{\mathrm{d}\mathbf{A}} = [0, I]^\top \ , \tag{4.9}$$

where I is the $dn_c \times dn_c$ identity matrix.

Let J^n be the Jacobian and solve numerically a coupled system of equations

$$J^{n+1} = J^n + \Delta t \frac{\mathrm{d}\mathbf{f}(\mathbf{X}^n)}{\mathrm{d}\mathbf{X}^n} J^n, \qquad \mathbf{X}^{n+1} = \mathbf{X}^n + \Delta t \mathbf{f}(\mathbf{X}^n) \tag{4.10}$$

with initial conditions $J^0 = [0, I]^\top, \mathbf{X}^0 = \mathbf{Y}$. In our problem, we have

$$\mathbf{f}(\mathbf{X}) = \begin{bmatrix} \frac{\partial H}{\partial \mathbf{q}} \\ -\frac{\partial H}{\partial \boldsymbol{\alpha}} \end{bmatrix}, \quad \mathbf{X} = \begin{bmatrix} \mathbf{q} \\ \boldsymbol{\alpha} \end{bmatrix}, \quad \frac{\mathrm{d}\mathbf{f}(\mathbf{X}^n)}{\mathrm{d}\mathbf{X}^n} = \begin{bmatrix} \frac{\partial^2 H}{\partial \mathbf{q} \partial \boldsymbol{\alpha}} & \frac{\partial^2 H}{\partial \boldsymbol{\alpha}^2} \\ -\frac{\partial^2 H}{\partial \mathbf{q}^2} & -\frac{\partial^2 H}{\partial \boldsymbol{\alpha} \partial \mathbf{q}} \end{bmatrix}. \tag{4.11}$$

The entries of the Jacobian in (4.11) can be calculated explicitly. The analytic calculation of the Jacobian permits efficient solution of the nonlinear equation $\Phi(\mathbf{A}; \mathbf{P}) = \mathbf{Q}$ using the nonlinear iterative solver `nag_nlin_sys_sol` developed by the Numerical Algorithms Group (NAG) [16]. The solver is based on MINPACK routines, described in [15].

We calculate the entries of (4.11). We have

$$\begin{aligned} H(\boldsymbol{\alpha}, \mathbf{q}) &= \frac{1}{2} \sum_{i,j=1}^{n_c} \boldsymbol{\alpha}_i^\top \boldsymbol{\alpha}_j G(\mathbf{q}_i, \mathbf{q}_j) \\ &= \sum_{i<j} \boldsymbol{\alpha}_i^\top \boldsymbol{\alpha}_j G(\mathbf{q}_i, \mathbf{q}_j) + \frac{1}{2} \sum_{i=1}^{n_c} \boldsymbol{\alpha}_i^\top \boldsymbol{\alpha}_i G(\mathbf{q}_i, \mathbf{q}_i), \end{aligned}$$

where we use the notation $\sum_{i<j}$ to denote summation from 1 to n_c such that $i < j$. We obtain first order derivatives

$$\frac{\partial H}{\partial \boldsymbol{\alpha}_k} = \sum_{j=1}^{n_c} \boldsymbol{\alpha}_j G(\mathbf{q}_k, \mathbf{q}_j), \tag{4.12}$$

$$\frac{\partial H}{\partial \mathbf{q}_k} = \sum_{i \neq k} \boldsymbol{\alpha}_i^\top \boldsymbol{\alpha}_k \frac{\partial G(\mathbf{q}_i, \mathbf{q}_k)}{\partial \mathbf{q}_k} + \frac{1}{2} \boldsymbol{\alpha}_k^\top \boldsymbol{\alpha}_k \frac{\partial G(\mathbf{q}_k, \mathbf{q}_k)}{\partial \mathbf{q}_k}. \tag{4.13}$$

Then we can calculate second derivatives

$$\frac{\partial^2 H}{\partial \boldsymbol{\alpha}_k \partial \boldsymbol{\alpha}_l} = G(\mathbf{q}_k, \mathbf{q}_l) I, \tag{4.14}$$

$$\frac{\partial^2 H}{\partial \boldsymbol{\alpha}_k \partial \mathbf{q}_l} = \boldsymbol{\alpha}_l \frac{\partial G(\mathbf{q}_k, \mathbf{q}_l)}{\partial \mathbf{q}_l}, \tag{4.15}$$

$$\frac{\partial^2 H}{\partial \boldsymbol{\alpha}_k \partial \mathbf{q}_k} = \sum_{j=1}^{n_c} \boldsymbol{\alpha}_j \frac{\partial G(\mathbf{q}_k, \mathbf{q}_j)}{\partial \mathbf{q}_k}, \tag{4.16}$$

$$\frac{\partial^2 H}{\partial \mathbf{q}_k \partial \mathbf{q}_l} = \boldsymbol{\alpha}_k^\top \boldsymbol{\alpha}_l \frac{\partial^2 G(\mathbf{q}_k, \mathbf{q}_l)}{\partial \mathbf{q}_k \partial \mathbf{q}_l}, \tag{4.17}$$

$$\frac{\partial^2 H}{\partial \mathbf{q}_k \partial \mathbf{q}_k} = \boldsymbol{\alpha}_k^\top \boldsymbol{\alpha}_k \frac{\partial^2 G(\mathbf{q}_k, \mathbf{q}_k)}{\partial \mathbf{q}_k \partial \mathbf{q}_k}, \tag{4.18}$$

(where I is the d-dimensional identity matrix). Then we can step forward using the Forward Euler scheme (4.10) to find control point paths for the system. Using this method, a 123 point test set was solved in less than 40 seconds using a single processor desktop computer.

5 Homeomorphic and diffeomorphic properties under numerical approximation

We investigate the homeomorphic and diffeomorphic qualities of, first continuous, and then discretized mappings.

The deformation field, $\mathbf{v}$, defines a mapping, Φ, which we show to be homeomorphic in the case $d = 2$. We define a continuous mapping based on the differential equation which defines the constraint, which we show to be well defined and continuous with continuous inverse. Before proceeding, we show an important inequality.

Proposition 3 *The minimizing deformation field $\mathbf{v} \in V$ is Lipschitz continuous so that for some $K > 0$, we have*

$$\|\mathbf{v}(\mathbf{x}, t) - \mathbf{v}(\mathbf{y}, t)\|_{\mathbb{R}^d} \leq K \|\mathbf{x} - \mathbf{y}\|_{\mathbb{R}^d}, \qquad 0 \leq t \leq 1, \qquad \mathbf{x}, \mathbf{y} \in \Omega.$$

Proof We have a representation for $\mathbf{v}$ (3.5) from Theorem 5 in terms of $\boldsymbol{\alpha}_i(t), \mathbf{x}_i(t), i = 1, \ldots, n_c$. The Green's function is globally Lipschitz continuous for $d = 2$, and the coefficients are continuous on a compact domain and so bounded. Hence we see that $\mathbf{v}$ is Lipschitz continuous. □

We examine the differential equation

$$\frac{\mathrm{d}\mathbf{x}_i(t)}{\mathrm{d}t} = \mathbf{v}(\mathbf{x}_i(t), t), \qquad \mathbf{x}_i(0) = \mathbf{P}_i, \qquad \mathbf{x}_i(t) \in \Omega, \tag{5.1}$$

with $\mathbf{v} \in V$. Define a mapping $\Phi : \Omega \to \Omega$ such that $\Phi(\mathbf{P}_i) = \mathbf{x}_i(1),\ i = 1, \ldots, n_c$. This mapping is a homeomorphism from $\Omega \to \Omega$.

By standards arguments (see, for instance [18]), we see that Φ defines a diffeomorphism on the domain, Ω.

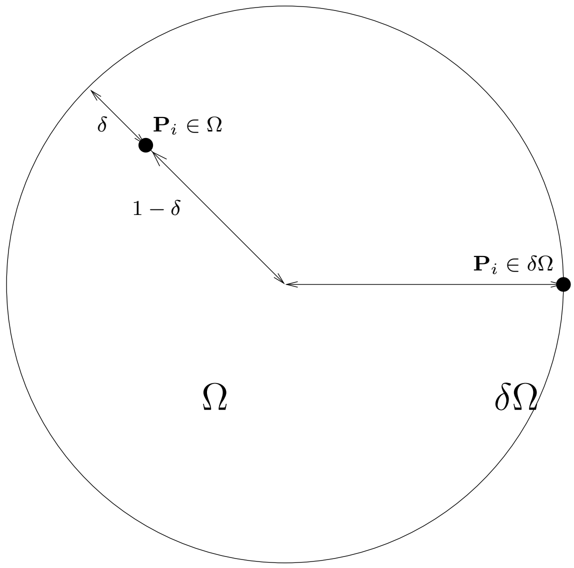

FIGURE 1. Visualization of the Proof of Theorem 6

We discretize the mapping for the purposes of computation. We need to be certain that the mapping will retain its diffeomorphic quality under this discretization.

We define a discretized mapping which we show to be well defined, by the Contraction Mapping Theorem, and to be continuous with a well defined, continuous inverse and hence show the discretized mapping to be a homeomorphism on a unit ball, Ω in the case $d = 2$. We can then see by the Inverse Mapping Theorem that the discretized mapping is diffeomorphic.

We examine the mapping, $\Phi_{\Delta t}$, where $\Phi_{\Delta t}$ is a time one mapping calculated using a Forward Euler numerical scheme with N time steps of size Δt, where $N\Delta t = 1$. We use the notation $\Phi^n_{\Delta t}(X)$ to denote X^n, the value of the n^{th} time step mapping. Then we have

$$\Phi^{n+1}_{\Delta t}(\mathbf{P}_i) = \Phi^n_{\Delta t}(\mathbf{P}_i) + \Delta t\, \mathbf{v}(\Phi^n_{\Delta t}(\mathbf{P}_i), n\Delta t), \qquad i = 1, \ldots, n_c,\ \mathbf{P}_i \in \Omega. \tag{5.2}$$

Theorem 6 *The mapping $\Phi_{\Delta t} : \Omega \to \Omega$ is a diffeomorphism for $\Delta t < \frac{1}{K}$, where K is the Lipschitz constant of the deformation field $\mathbf{v}$, recalling that $\mathbf{v}$ is Lipschitz continuous by Proposition 3 and has zero Dirichlet boundary conditions on $\delta\Omega$ where Ω is the unit ball.*

Proof We consider two cases, as shown in Figure 1. First, we show that $\Phi_{\Delta t}$ maps from Ω into Ω.

In the first case, suppose $\mathbf{P}_i \in \partial\Omega$. Then $\Phi^{n+1}_{\Delta t}(\mathbf{P}_i) = \Phi^n_{\Delta t}(\mathbf{P}_i)$ due to the boundary conditions, and so clearly we have $\Phi^{n+1}_{\Delta t}(\mathbf{P}_i) \in \Omega$.

Now we examine the more general case, $\Phi^n_{\Delta t}(\mathbf{P}_i) \in \Omega$. Applying the triangle inequality for norms to (5.2), we can write

$$\|\Phi^{n+1}_{\Delta t}(\mathbf{P}_i)\|_{\mathbb{R}^d} \leq \|\Phi^n_{\Delta t}(\mathbf{P}_i)\|_{\mathbb{R}^d} + \Delta t \|\mathbf{v}(\Phi^n_{\Delta t}(\mathbf{P}_i), n\Delta t)\|_{\mathbb{R}^d}.$$

The Lipschitz continuity of $\mathbf{v}$ gives

$$\|\mathbf{v}(\Phi_1, s) - \mathbf{v}(\Phi_2, s)\|_{\mathbb{R}^d} \le K\|\Phi_1 - \Phi_2\|_{\mathbb{R}^d}, \qquad K < \infty,\ \ \Phi_1, \Phi_2 \in \Omega,\ \ 0 \le s \le 1,$$

and so we can write

$$\left\| \mathbf{v}\left(\frac{\Phi^n_{\Delta t}(\mathbf{P}_i)}{\|\Phi^n_{\Delta t}(\mathbf{P}_i)\|_{\mathbb{R}^d}}, s\right) - \mathbf{v}(\Phi^n_{\Delta t}(\mathbf{P}_i), s)\right\|_{\mathbb{R}^d} \le K \left\| \frac{\Phi^n_{\Delta t}(\mathbf{P}_i)}{\|\Phi^n_{\Delta t}(\mathbf{P}_i)\|_{\mathbb{R}^d}} - \Phi^n_{\Delta t}(\mathbf{P}_i)\right\|_{\mathbb{R}^d}.$$

Since we know $\frac{\Phi^n_{\Delta t}(\mathbf{P}_i)}{\|\Phi^n_{\Delta t}(\mathbf{P}_i)\|_{\mathbb{R}^d}} \in \partial\Omega$, we have $\mathbf{v}\left(\frac{\Phi^n_{\Delta t}(\mathbf{P}_i)}{\|\Phi^n_{\Delta t}(\mathbf{P}_i)\|_{\mathbb{R}^d}}, s\right) = 0$, so we have

$$\|\mathbf{v}(\Phi^n_{\Delta t}(\mathbf{P}_i), s)\|_{\mathbb{R}^d} \le K \left\| \frac{\Phi^n_{\Delta t}(\mathbf{P}_i)}{\|\Phi^n_{\Delta t}(\mathbf{P}_i)\|_{\mathbb{R}^d}} - \Phi^n_{\Delta t}(\mathbf{P}_i)\right\|_{\mathbb{R}^d}.$$

Hence we have

$$\|\Phi^{n+1}_{\Delta t}(\mathbf{P}_i)\|_{\mathbb{R}^d} \le \|\Phi^n_{\Delta t}(\mathbf{P}_i)\|_{\mathbb{R}^d} + K\Delta t \left\| \frac{\Phi^n_{\Delta t}(\mathbf{P}_i)}{\|\Phi^n_{\Delta t}(\mathbf{P}_i)\|_{\mathbb{R}^d}} - \Phi^n_{\Delta t}(\mathbf{P}_i)\right\|_{\mathbb{R}^d}.$$

Now, without loss of generality, suppose $\|\Phi^n_{\Delta t}(\mathbf{P}_i)\|_{\mathbb{R}^d} = 1 - \delta,\ \delta > 0$.
We have $\left\|\frac{\Phi^n_{\Delta t}(\mathbf{P}_i)}{\|\Phi^n_{\Delta t}(\mathbf{P}_i)\|_{\mathbb{R}^d}}\right\|_{\mathbb{R}^d} = 1$, so we can write

$$\begin{aligned}\|\Phi^{n+1}_{\Delta t}(\mathbf{P}_i)\|_{\mathbb{R}^d} &\le 1 - \delta + K\Delta t(1 - (1 - \delta)) \\ &\le 1 - \delta + K\Delta t\delta.\end{aligned}$$

Since $\Phi^{n+1}_{\Delta t}(\mathbf{P}_i) \in \Omega$ for $\|\Phi^{n+1}_{\Delta t}(\mathbf{P}_i)\|_{\mathbb{R}^d} \le 1$, we see that $\Phi^{n+1}_{\Delta t}(\mathbf{P}_i) \in \Omega$ for

$$\begin{aligned}1 - \delta + K\Delta t\delta &\le 1 \\ K\Delta t\delta &\le \delta \\ K\Delta t &\le 1.\end{aligned}$$

Hence we conclude $\Phi_{\Delta t} : \Omega \to \Omega$ for $\Delta t \le \frac{1}{K}$, meaning that the behaviour of the required Δt is independent of the position of the points, and only depends on the Lipschitz constant of the function, $\mathbf{v}$.

We see that $\Phi_{\Delta t}$ has a unique solution by the same argument as that for the non-discretized case. Now we show $\Phi_{\Delta t}$ to be continuous. We adapt a proof from Stuart and Humphries [18].

Suppose we have points $\mathbf{P}_1, \mathbf{P}_2 \in \Omega$. Then, at the first time step, we have $\Phi^1_{\Delta t}(\mathbf{P}_1) = \mathbf{P}_1 + \mathbf{v}(\mathbf{P}_1, 0), \Phi^1_{\Delta t}(\mathbf{P}_2) = \mathbf{P}_1 + \mathbf{v}(\mathbf{P}_2, 0)$, and so

$$\begin{aligned}\|\Phi^1_{\Delta t}(\mathbf{P}_1) - \Phi^1_{\Delta t}(\mathbf{P}_2)\|_{\mathbb{R}^d} &\le \|\mathbf{P}_1 - \mathbf{P}_2\|_{\mathbb{R}^d} + \Delta t\|\mathbf{v}(\mathbf{P}_1, 0) - \mathbf{v}(\mathbf{P}_2, 0)\|_{\mathbb{R}^d} \\ &\le \|\mathbf{P}_1 - \mathbf{P}_2\|_{\mathbb{R}^d} + K\Delta t\|\mathbf{P}_1 - \mathbf{P}_2\|_{\mathbb{R}^d} \\ &\le (K\Delta t + 1)\|\mathbf{P}_1 - \mathbf{P}_2\|_{\mathbb{R}^d} \qquad (5.3)\end{aligned}$$

where K is the Lipschitz constant for $\mathbf{v}$. Hence $\Phi_{\Delta t}$ is continuous for the first time step and similarly will be continuous over all N time steps.

We define an inverse mapping $\Psi^n_{\Delta t}$ such that $\Psi^0_{\Delta t}(\mathbf{Q}_i) = \mathbf{Q}_i$ and such that $\Psi^N_{\Delta t}(\mathbf{Q}_i) = \mathbf{P}_i,\ i = 1, \ldots, n_c$. This inverse mapping is generated by the Backward Euler scheme

$$\Psi^{n+1}_{\Delta t}(\mathbf{Q}_i) = \Psi^n_{\Delta t}(\mathbf{Q}_i) - \Delta t\mathbf{v}(\Psi^{n+1}_{\Delta t}(\mathbf{Q}_i), (n + 1)\Delta t).$$

First, we show that this mapping is well defined.

We can define a mapping, $\mathcal{M}$, as

$$\mathcal{M}(\Psi) = \mathbf{Q}_i + \Delta t \mathbf{v}(\Psi, n\Delta t).$$

In order to use the Contraction Mapping Theorem, we show $\mathcal{M}$ to be a contraction. Suppose we have two points $\Psi_1, \Psi_2 \in \Omega$. Then we can write

$$\begin{aligned}\|\mathcal{M}(\Psi_1) - \mathcal{M}(\Psi_2)\|_{\mathbb{R}^d} &= \|\mathbf{Q}_i - \mathbf{Q}_i + \Delta t(\mathbf{v}(\Psi_1, s) - \mathbf{v}(\Psi_2, s)\|_{\mathbb{R}^d}, \\ &\leq \Delta t K \|\Psi_1 - \Psi_2\|_{\mathbb{R}^d} \text{ by Lipschitz continuity of } \mathbf{v}.\end{aligned}$$

Hence we see that $\mathcal{M}$ defines a contraction, and so $\Psi_{\Delta t}$ is well-defined, for $\Delta t K < 1$. Following the approach of Stuart [18], we show that $\Psi_{\Delta t}$ is a continuous mapping for $\Delta t \leq \frac{1}{K}$. Consider Backward Euler iterations

$$\Psi^{n+1}_{\Delta t}(\mathbf{Q}_i) = \Psi^{n}_{\Delta t}(\mathbf{Q}_i) - \Delta t \mathbf{v}(\Psi^{n+1}_{\Delta t}(\mathbf{Q}_i), (n+1)\Delta t),$$

along with a second set of iterations given by

$$\Upsilon^{n+1}_{\Delta t}(\mathbf{Q}_i) = \Upsilon^{n}_{\Delta t}(\mathbf{Q}_i) - \Delta t \mathbf{v}(\Upsilon^{n+1}_{\Delta t}(\mathbf{Q}_i), (n+1)\Delta t).$$

Then we have

$$\|\Psi^{n+1}_{\Delta t}(\mathbf{Q}_i) - \Upsilon^{n+1}_{\Delta t}(\mathbf{Q}_i)\|_{\mathbb{R}^d} \leq \|\Psi^{n}_{\Delta t}(\mathbf{Q}_i) - \Upsilon^{n}_{\Delta t}(\mathbf{Q}_i)\|_{\mathbb{R}^d} + \Delta t K \|\Psi^{n+1}_{\Delta t}(\mathbf{Q}_i) - \Upsilon^{n+1}_{\Delta t}(\mathbf{Q}_i)\|_{\mathbb{R}^d},$$

using the Lipschitz continuity of $\mathbf{v}$. Then, since $\Delta t < \frac{1}{K}$, we can write

$$\|\Psi^{n+1}_{\Delta t}(\mathbf{Q}_i) - \Upsilon^{n+1}_{\Delta t}(\mathbf{Q}_i)\| \leq \frac{1}{1 - K\Delta t} \|\Psi^{n}_{\Delta t}(\mathbf{Q}_i) - \Upsilon^{n}_{\Delta t}(\mathbf{Q}_i)\|. \tag{5.4}$$

So we see that the inverse mapping is continuous.

Hence we conclude that $\Phi_{\Delta t}$ with $\Delta t < \frac{1}{K}$ is homeomorphic on Ω.

From (5.3) and (5.4), we see that the Jacobians of the mapping and the inverse mapping are bounded. Hence, by the Inverse Mapping Theorem, we conclude that the mapping is also diffeomorphic. □

6 Uniqueness of paths - proof and numerical example

We have shown that minimizing velocity fields and paths exist for the Geodesic Interpolating Spline problem, and have shown that the velocity field generated by minimizing paths is unique. It should be noted, however that the minimizing paths are not always unique, as there can be symmetric minimizing paths, which will be demonstrated by numerical experiment, and shown in Proposition 4.

Proposition 4 *There exist combinations of start points, $\mathbf{P}_i$, and end points, $\mathbf{Q}_i$, for which there is not a unique minimizer to the problem of Theorem 1.*

Proof Suppose we have a set of two start points, $\mathbf{P}_1, \mathbf{P}_2 \in \Omega$ and two corresponding end points, $\mathbf{Q}_1, \mathbf{Q}_2 \in \Omega$ with reflective symmetry about the x-axis so that we have $\mathbf{P}_1 = (-a, b), \mathbf{P}_2 = (-a, -b), \mathbf{Q}_1 = (a, -b), \mathbf{Q}_2 = (a, b)$, as illustrated in Figure 2.

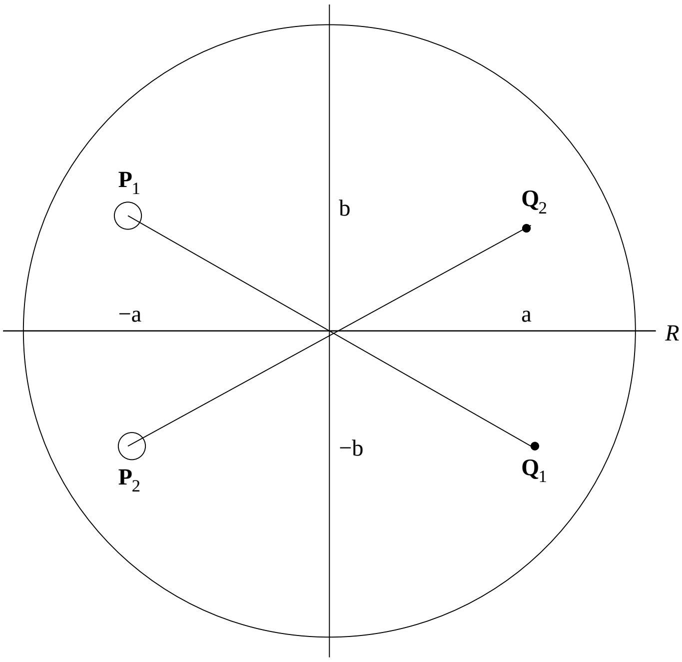

FIGURE 2. Illustration of Symmetric Start and End Points

Suppose, toward a contradiction, that we have unique minimizing paths $\mathbf{x}_1, \mathbf{x}_2$ such that

$$\mathbf{x}_1(0) = \mathbf{P}_1 = R\mathbf{P}_2 = R\mathbf{x}_2(0)$$

and

$$\mathbf{x}_1(1) = \mathbf{Q}_1 = R\mathbf{Q}_2 = R\mathbf{x}_2(1),$$

where R is an operator indicating reflection about the x-axis.

The uniqueness of minimizing paths implies that we must have $\mathbf{x}_1(t) = R\mathbf{x}_2(t)\ \forall t \in [0,1]$. Consider the point where the path $\mathbf{x}_1$ crosses the y-axis at, say $\mathbf{x}_1(\tau) = (\alpha, 0),$ some $\tau \in (0,1), \alpha \in [0,1]$. At this point we must have $\mathbf{x}_2(\tau) = (\alpha, 0) = R\mathbf{x}_2(\tau)$. Hence we have $\mathbf{x}_1(\tau) = \mathbf{x}_2(\tau)$. This is impossible since we have uniqueness of solution to the differential equations initialized from any point. Hence if we have $\mathbf{x}_1(\tau) = \mathbf{x}_2(\tau)$, we cannot have $\mathbf{x}_1(1) = \mathbf{Q}_1$ and $\mathbf{x}_2(1) = \mathbf{Q}_2$, since $\mathbf{Q}_1$ and $\mathbf{Q}_2$ are not coincident.

Hence we conclude that there are not always unique minimizing paths for a set of start points and end points. □

There are special cases for which there are symmetric solutions of paths. To force the shooting method to find these symmetric solutions, we experiment with the choice of initial data for $\boldsymbol{\alpha}$.

We examine the paths for a test problem with two initial knot point positions, $(0.2, -0.2)$ and $(-0.2, -0.2)$ moving to final positions, $(-0.2, 0.2)$ and $(0.2, 0.2)$, respectively. First, the initial $\boldsymbol{\alpha}$ multipliers are set to 1, the default for the routine. The shooting method solver then outputs a set of final values for $\boldsymbol{\alpha}$, producing the paths shown on the left

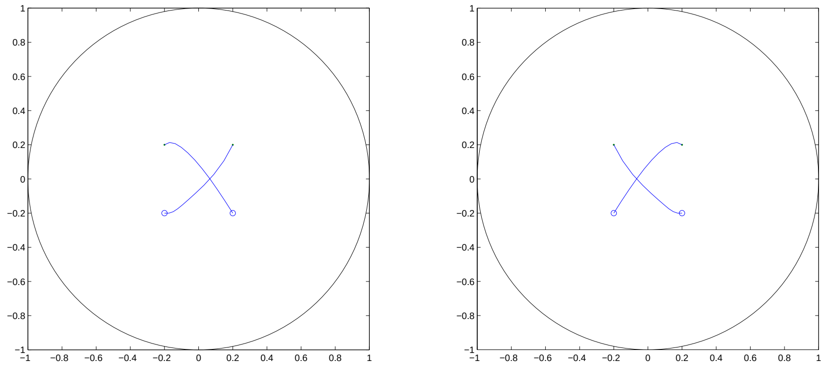

FIGURE 3. Symmetry Created By Changing the Initial Conditions for the Shooting Method From $\boldsymbol{\alpha}$ to -$\boldsymbol{\alpha}$

hand side of Figure 3. We then initialize the solver with $-\boldsymbol{\alpha}$. This produces the paths shown on the right hand side of Figure 3. Experiments where all elements of $\boldsymbol{\alpha}$ and $-\boldsymbol{\alpha}$ were initialized as either -1 or 1, according to the sign of the original element produced exactly the same paths as those produced by initializing with $\boldsymbol{\alpha}$ and $-\boldsymbol{\alpha}$.

We have shown uniqueness of the velocity field generated from a given set of paths in Section 2. This experiment shows that the paths that minimize the problem are not always unique since they have symmetric equivalents for certain configurations, but from Section 2, we know that once a path has been selected from a set of symmetrically equivalent paths, there is only one possible velocity field to be generated.

7 Conclusion

We have extended a previous result for inexact landmark-matching to show that for exact landmark-matching the minimizing paths for GIS exist, with corresponding unique vector fields. We have adapted techniques from approximation theory to show that the velocity fields can be expanded as a finite linear combination of Green's functions without introducing any approximation. We have proved that, under sufficiently small time steps, the discrete GIS mappings are diffeomorphic, as was previously believed to be the case.

References

[1] T. BOGGIO, *Sulle funzioni di green d'ordine m.*, Rend. Circ. Matem. Palermo, 20 (1905), pp. 97–135.

[2] F. BOOKSTEIN, *Principal warps: thin-plate splines and the decomposition of deformations*, IEEE Transactions on Pattern Analysis and Machine Intelligence, 11 (1989), pp. 567–585.

[3] V. CAMION AND L. YOUNES, *Geodesic interpolating splines*, in M.A.T. Figueiredo, J. Zerubia, A K. Jain ed., vol. 2134 of Energy Minimization Methods in Computer Vision and Pattern Recognition, Lecture notes in Computer Science, Springer-Verlag, 2001, pp. 513–527.

[4] W. CHENEY AND W. LIGHT, *A course in approximation theory*, Brooks/Cole, 1999.

[5] M. do Carmo, *Differential geometry of curves and surfaces*, Prentice-Hall, Inc., Englewood Cliffs, New Jersey, 1976.

[6] P. Dupuis, U. Grenander, and M. Miller, *Variational problems on flows of diffeomorphism for image matching*, Quarterly of Applied Mathematics, LVI (1998), pp. 587–600.

[7] H. Johnson and G. Christensen, *Consistent landmark and intensity based image registration*, IEEE Transactions on Medical Imaging, 21 (2002).

[8] S. Joshi and M. Miller, *Landmark matching via large deformation diffeomorphisms*, IEEE Transactions on Image Processing, 9 (2000).

[9] S. L. Keeling and W. Ring, *Medical image registration and interpolation by optical flow with maximal rigidity*, Journal of Mathematical Imaging and Vision, 23 (2005), pp. 47–65.

[10] B. Leimkuhler and S. Reich, *Simulating Hamiltonian dynamics*, Cambridge University Press, 2004.

[11] S. Marsland and C. Twining, *Measuring geodesic distances on the space of bounded diffeomorphisms*, in British Machine Vision Conference (BMVC), 2002.

[12] A. Mills, *Optimizing the paths for geodesic interpolating splines*, master's thesis, University of Manchester, 2003.

[13] A. Mills, T. Shardlow, and S. Marsland, *Computing the geodesic interpolating spline*, in Biomedical Image Registration, Third International Workshop, WBIR 2006, vol. 4057 of Lecture Notes in Computer Science, Springer, 2006, pp. 169–177.

[14] J. Modersitzki, *Numerical methods for image registration*, Oxford University Press, New York, 2004.

[15] J. J. Moré, B. S. Garbow, and K. E. Hillstrom, *User guide for MINPACK–1*, Technical Report ANL–80–74, Mathematics and Computer Sciences Division, Argonne National Laboratory, Argonne, Ill., 1980.

[16] Numerical Algorithms Group, *NAG Manual*, http://www.nag.co.uk/numeric/FN/manual/.

[17] M. Renardy and R. Rogers, *An introduction to partial differential equations*, Springer Verlag, 1996.

[18] A. Stuart and A. Humphries, *Dynamical systems and numerical analysis*, vol. 2 of Cambridge monographs on applied and computational mathematics, Cambridge University Press, 1996.